Biophys Struct Mech (1984) 10 : 241–256

Biophysics of Structure and Mechanism

Investigation of pH-Induced Symmetry Distortions of the Prosthetic Group in Deoxyhaemoglobin by Resonance Raman Scattering

R. Schweitzer-Stenner, W. Dreybrodt, and S. el Naggar

Universität Bremen, Fachbereich 1 – Physik, D-2800 Bremen 33, Federal Republic of Germany

Abstract. The depolarization ratio and the excitation profiles of the Raman line at 1,355 cm^{-1} (oxidation marker) of deoxyhaemoglobin show a significant dispersion in the region between the α- and Soret-band, which is drastically dependent on the pH-value of the solution. The experimental data are interpreted by extending the Loudon theory of the Raman tensor by introducing static distortions of the haem group, which result from haem-apoprotein interactions. Thus, a Raman tensor results as a linear combination of A_{1g}, A_{2g}, B_{1g}, B_{2g} Raman tensors in D_{4h}-symmetry. By fitting the data to this expression, constants are obtained which are related linearly to symmetry classified distortions of the haem group. The variation of all these distortions shows a similar pH-dependence, which is interpreted to be caused by protonation processes of two titrable groups with $pK_1 = 4.3$ and $pK_2 = 5.4$.

Key words: Deoxyhaemoglobin – Resonance Raman scattering – Dispersion of depolarization ratio – Symmetry distortions – Bohr effect

Introduction

The structural properties of the prosthetic group of several haem proteins and their dependence on interactions between the haem and the apoprotein via the Fe^{2+}-*His*(F8) bond have been examined by many resonance Raman experiments during the last few years (Burke et al. 1978; Kincaid et al. 1979; Scholler and Hoffmann 1979; Shelnutt et al. 1979; Nagai et al. 1980; Debois et al. 1981a, 1981b; Ondrias et al. 1982; Tsubaki et al. 1982; Valance and Strekas 1982). A systematic investigation, however, dealing with symmetry distortions of the haem group induced by variation of the tertiary and quarterary structure of the globular protein, has not yet been reported.

Investigations of the dispersion of the depolarization ratio (DPR) and the excitation profiles (EPS) of Raman lines of porphyrin and haem protein spectra have been shown to be suitable tools for detecting symmetry-lowering distortions of the haem group from its ideal D_{4h}-symmetry (Collins et al. 1973; Verma

et al. 1974; Mendelsohn et al. 1975; Verma and Bernstein 1974; Sunder et al. 1975; Plus and Lutz 1974; Debois et al. 1979). Shelnutt (1979) gives a theoretical interpretation of the dispersive behaviour of the DPR in the resonant region of the Q-bands of porphyrin spectra, assuming an additional perturbation potential in the Herzberg-Teller expansion of the polarizibility tensor. Hennecker et al. (1978a and b), and Zgierski and Pawlikowski (1978, 1981, 1982) extend this theoretical interpretation, taking into consideration degeneracy splitting of the Q- and B-states, vibrational and electronic perturbation. This theory, however, from the computational point of view, is rather complicated, that, so far, a systematic parametrization of experimental depolarization curves and the corresponding excitation profiles of haem protein Raman spectra has not yet been given.

In a previous work, Schweitzer et al. (1982) found a significant pH dependence of the depolarization curves of the 1,375 cm^{-1}, 1,583 cm^{-1}, and 1,638 cm^{-1} Raman lines of the oxyhaemoglobin spectra between β- and Soret band in the physiological region between pH = 6.0 and 8.0. Since the alkaline Bohr effect is maximal between 7.0 and 8.0, one may conclude that the protonation of Bohr groups causes a variation of the haem group symmetry, which is reflected by a variation of the DPR dispersion curves and EPS.

In this paper we report measurements and analysis of the DPR dispersion curves and the excitation profiles of the 1,355 cm^{-1} oxidation marker-line of the deoxyspectrum for different pH-values between pH = 2.0 and pH = 8.0. Our results show a characteristic pH-dependence of different symmetry-classified distortions of the haem. We are able to explain this behaviour by assuming that the protonation state of two titrable groups of the globular protein has a significant influence on the prosthetic group via haem-apoprotein contacts.

Theoretical Background

Collins et al. (1973), in a first approach to understand the frequency dependence of the DPR in haem proteins by using PNSF theory (Loudon 1973; Peticolas et al. 1970), have given the following expression for the polarizibility tensor of the porphyrin system

$$\hat{\beta}(\tilde{\nu}_L, \tilde{\nu}_R, \tilde{\nu}_Q, \tilde{\nu}_B) = \alpha_{QB}^{A_{2g}} \hat{\Gamma}^{A_{2g}} F_{QB}^{\tilde{a}}(\tilde{\nu}_L, \tilde{\nu}_R, \tilde{\nu}_Q, \tilde{\nu}_B) + \sum_{e,s} \left\{ \left(\sum_{\Gamma} \alpha_{es}^{\Gamma} \hat{\Gamma}^{\Gamma} \right) F_{es}^{\tilde{s}}(\tilde{\nu}_e, \tilde{\nu}_s) \right\} \tag{1a}$$

e, s are wave-number indices for the electronic transition related to the α-band (Q) and the Soret band (B).

$$F_{es}^{\tilde{s},\tilde{a}} = \frac{1}{(\tilde{\nu}_e + \tilde{\nu}_R - \tilde{\nu}_L + i\gamma^e)(\tilde{\nu}_s - \tilde{\nu}_L + i\gamma^s)} + \frac{1}{(\tilde{\nu}_e - \tilde{\nu}_R + \tilde{\nu}_L + i\gamma^e)(\tilde{\nu}_s + \tilde{\nu}_L + i\gamma^s)} \pm \frac{1}{(\tilde{\nu}_e - \tilde{\nu}_L + i\gamma^e)(\tilde{\nu}_s + \tilde{\nu}_R - \tilde{\nu}_L + i\gamma^s)} \pm \frac{1}{(\tilde{\nu}_e + \tilde{\nu}_L + i\gamma^e)(\tilde{\nu}_s - \tilde{\nu}_R + \tilde{\nu}_L + i\gamma^s)} \tag{1b}$$

$\tilde{\nu}_L$ = laser wave number
$\tilde{\nu}_e$, $\tilde{\nu}_s$ = electronic transition wave number
$\tilde{\nu}_R$ = Raman wave number
α_{es}^{Γ} = complex constants for each tensor T^{Γ} of the representation Γ as tabulated by McClain (1971) for D_{4h}-symmetry
γ^e, γ^s = halfwidth of the electronic levels (e) and (s)

The tensor $\hat{\beta}$ is a linear combination of tensors according to all Raman-allowed vibrational modes, i.e., A_{1g}, B_{1g}, A_{2g}, B_{2g}. Collins et al. (1973) were thus able to fit their experimental data of DPR in cytochromic. By this procedure they obtained the constants α_{es}^{Γ} as parameters. Once these parameters are known, one is able to calculate all the properties of the Raman lines, since the constants α_{es}^{Γ} determine all the components of the Raman tensor over the whole range of wave numbers.

Especially from the fit of the DPR dispersion curves one should be able to predict the excitation profiles of the Raman line. Thus, the formula of Collins et al. (1973) is a promising tool for obtaining detailed information from an easily measurable property. Its shortcoming, however, is that so far no physical interpretation of the fitting parameters has been given. Collins only indicates that the reason for admixing of the different vibrational modes may be due to a perturbation of D_{4h}-symmetry.

Starting at that point, we assume that the molecule is somehow distorted by δq from its ideal D_{4h}-symmetry. Every distortion of a molecule can be described by a superposition of normal coordinates. Thus:

$$\delta q = \sum_j \delta Q_j \,, \tag{2}$$

where δQ_j is a distortion from the unperturbed state parallel to the normal coordinate of the j-th normal vibration in D_{4h}-symmetry.

In the following we introduce this assumption into the PNSF theory for Raman scattering, which was developed by Peticolas et al. (1970), using third order perturbation theory according to Loudon (1973). They work out the following equation for the Resonance Raman scattering tensor:

$$\begin{aligned}\hat{\beta}_{\varrho\sigma} = \sum_{e,\,s} [&\mathcal{M}_{\varrho}^{ge} H_{es}^{R} \mathcal{M}_{\sigma}^{gs} \{(\tilde{\nu}_e + \tilde{\nu}_R - \tilde{\nu}_L + i\gamma^e)(\tilde{\nu}_s - \tilde{\nu}_L + i\gamma^s)\}^{-1} \\ &+ \mathcal{M}_{\sigma}^{ge} H_{es}^{R} \mathcal{M}_{\varrho}^{gs} \{(\tilde{\nu}_e - \tilde{\nu}_R + \tilde{\nu}_L + i\gamma^e)(\tilde{\nu}_s + \tilde{\nu}_L + i\gamma^s)\}^{-1} Q_R^{01}\end{aligned} \tag{3}$$

$\mathcal{M}_{\varrho}^{g,e}$ = dipole transition matrix element
ϱ, σ = direction for the transition polarized in direction ϱ, σ from the ground state to the electronic state $|e\rangle$, $|s\rangle$: $\mathcal{M}_{\varrho}^{g,e} = \langle g|\mathbf{P}_{\varrho}|e\rangle$
H_{es}^{R} = matrix element of the vibrational coupling operator $\dfrac{\partial H}{\partial Q_R}$ between two excited electronic states $|e\rangle$ and $|s\rangle$ according to the normal coordinate Q_R of the R-th vibration: $\left\langle e \left| \dfrac{\partial H}{\partial Q_R} \right| s \right\rangle$
Q_R^{01} = vibronic transition matrix element between the 0-th and the 1-st vibrational level of the electronic ground state: $Q_R^{01} = \langle 0|Q_R|1\rangle$.

To obtain the Raman tensor of the distorted molecule one now has to replace the matrix element H_{es}^{R} in the expression of $\beta_{\varrho\sigma}^{R}$ by the corresponding matrix element in the distorted molecule. The distortion changes the unperturbed electronic states $|e\rangle, |s\rangle$ into perturbed states $|e'\rangle, |s'\rangle$.

The vibronic coupling operator is to be calculated at the new equilibrium position given by the distortion coordinates $\delta Q_1 \ldots \delta Q_j \ldots \delta Q_n$. Since the distortions are assumed to be small, an expansion to first order is possible.
Thus:

$$\left(\frac{\partial H}{\partial Q_R}\right)_{\text{dist}} = \frac{\partial H}{\partial Q_R}\Bigg|_{\delta Q_j = 0} + \sum_j \frac{\partial^2 H}{\partial Q_R\, \partial Q_j}\,\delta Q_j\,. \tag{4}$$

Introducing $\left(\frac{\partial H}{\partial Q}\right)_{\text{dist}}$ into Eq. (3), one obtains correct to second order

$$\begin{aligned}(\hat{\beta}_{\varrho,\sigma})_{\text{dist}} &= \hat{\beta}_{\varrho\sigma} \\ &+ \sum_j \sum_{e,\,s} \{\mathcal{M}_{\varrho}^{ge}\, H_{es}^{Rj}\, \mathcal{M}_{\varrho}^{gs}\, [(\tilde{\nu}_e + \tilde{\nu}_R - \tilde{\nu}_L + i\gamma^e)\,(\tilde{\nu}_s - \tilde{\nu}_L + i\gamma^s)]^{-1} \\ &+ \mathcal{M}_{\sigma}^{ge}\, H_{es}^{Rj}\, \mathcal{M}_{\varrho}^{gs}\, [(\tilde{\nu}_s - \tilde{\nu}_R + \tilde{\nu}_L + i\gamma^e)\,(\tilde{\nu}_e + \tilde{\nu}_L + i\gamma^e)]^{-1}\}\, Q_R^{01}\end{aligned} \tag{5}$$

$$H_{es}^{Rj} = \left\langle e \left| \frac{\partial^2 H}{\partial Q_R\, \partial Q_j} \right| s \right\rangle \delta Q_j\,.$$

$\beta_{\varrho\sigma}$ is the tensor of Eq. (3) transforming according to Q_R in the unperturbed symmetry D_{4h}, as given by McClain (1971).

The second term is a tensor transforming according to $\frac{\partial^2 H}{\partial Q_R\, \partial Q_j}$, i.e., $\Gamma_{QR} \times \Gamma_{Qj}$, Γ_{QR}, Γ_{Qj} are the representations of Q_R and Q_j respectively in D_{4h}-symmetry. Since in haemoglobin one obtains the Raman tensor by summing only over two excited states e, $s = Q$, B which both transform like E_u, the second order vibronic coupling element only gives contributions to $\hat{\beta}_{\text{dist}}$ if $\Gamma_{Qj} \times \Gamma_{QR}$ transforms like $E_u \times E_u = A_{1g} + B_{1g} + B_{2g} + A_{2g}$ in D_{4h}.

Thus, the tensor of the distorted molecule becomes a linear combination of all tensors of Raman active vibrations and the fitting constants α_{es}^{Γ} in the expression of Collins et al. (1973) are related linearly to the distortions δQ_j. The fitting parameters α_{es}^{Γ} are easily related from Eq. (1) to Eq. (5) by comparison of coefficients.

From the knowledge of the symmetry type Γ_T of the contributing tensors and that of the observed Raman line in D_{4h}-symmetry, one can conclude which symmetry types of distortions δQ_j are present, as $\Gamma_{Qj} \times \Gamma_{QR} = \Gamma_T$. Table 1 lists this multiplication for D_{4h}-symmetry.

We have used Eq. (1), i.e., Eq. (5) respectively to fit our experimental DPR curves of *deoxy*Hb. From the set of fitting parameters thus obtained, the excitation profiles were calculated and compared with the experimental results. If only poor agreement resulted, the fit parameters were slightly changed until good agreement was achieved.

Table 1. Correlation table of distortion symmetry type and vibrational symmetry of the Raman vibration in the undistorted D_{4h}-symmetry. The entities in the corresponding rows and columns give the symmetry type contributing to the Raman tensor

Vibration in undistorted molecule	Distortion				
	Q_a	Q_j			
		A_{1g}	B_{1g}	B_{2g}	A_{2g}
	A_{1g}	A_{1g}	B_{1g}	B_{2g}	A_{2g}
	B_{1g}	B_{1g}	A_{1g}	A_{2g}	B_{2g}
	B_{2g}	B_{2g}	A_{2g}	A_{1g}	B_{1g}
	A_{2g}	A_{2g}	B_{2g}	B_{1g}	A_{1g}

Thus, we were able to calculate simultaneously the DPR dispersion curves and the excitation profiles $I_{\perp,\parallel}$ and $I_{\perp,\perp}$. The first index in I represents the polarization of the incident beam relative to the scattering plane and the second one refers to the polarization of the Raman light.

First data were also taken on three Raman lines in *oxy*Hb reveal DPR and EPS of more complicated structure than those of *deoxy*Hb. Although a reasonable fit of the DPR dispersion could always be obtained, by use of Eq. (5), those fits did not reproduce the experimental data of EPS. This will be reported in detail in a future paper.

Because of the more complicated structure of *oxy*Hb and the fact that the absorption of *oxy*Hb shows clearly two Q-bands according to 0-0 and 0-1 transitions, we suspect that the vibronic structure of the Q-band has to be taken into account, in order to reproduce the experimental data of *oxy*Hb.

In the formalism of Peticolas et al. (1970) so far all transitions from the ground state $|g\rangle\,|0\rangle$ to vibronically excited states of modes other than the observed Raman mode $|Q\rangle\,|1_\mu\rangle$, $|B\rangle\,|1_\mu\rangle$ and Raman excitation induced by strong vibronic coupling in the region of the β-band have been neglected. To simulate such processes, we introduce additional 0-1 resonance terms for the Q- and B-state into the PNSF formalism, weighting them with constants C_{QQ}, C_{BB}, and C_{QB} which are related to Franck-Condon integrals of Q and B states and to vibronic coupling into the Q-state respectively. This leads to extra contributions into Eq. (5), which are different from those by energy denominators corresponding to the transitions $|g\rangle\,|0\rangle \rightarrow |Q\rangle\,|1_\mu\rangle$ and $|g\rangle\,|0\rangle \rightarrow |B\rangle\,|1_\mu\rangle$.

Thus we can formulate the equation for the polarizibility tensor $\hat{\beta}$, which has been used in the fitting program:

$$(\hat{\beta})_{\text{dist}} = \alpha_{QB}^{A_{2g}} \hat{\uparrow}^{A_{2g}} \{F_{QB}^{\tilde{\nu}} (\tilde{\nu}_Q, \tilde{\nu}_B) + C_{QB}^{\tilde{\nu}} F_{QB}^{\tilde{\nu}} (\tilde{\nu}_Q + \tilde{\nu}_\mu, \tilde{\nu}_B + \tilde{\nu}_\mu)\}$$
$$+ \sum_{e,s} \left\{ \left[\sum_{\Gamma} \alpha_{es}^{\Gamma} \hat{\uparrow}^{\Gamma} \right] [F_{es}^{\tilde{\nu}} (\tilde{\nu}_e, \tilde{\nu}_s) + C_{es}^{\tilde{\nu}} F_{es}^{\tilde{\nu}} (\tilde{\nu}_e + \tilde{\nu}_\mu, \tilde{\nu}_s + \tilde{\nu}_\mu)] \right\} \tag{6}$$

with

$$C_{QQ}^{\tilde{s}} = \frac{\langle 0_\mu^g | 1_\mu^Q \rangle \langle 1_\mu^Q | 0_\mu^g \rangle}{\langle 0_\mu^g | 0_\mu^Q \rangle \langle 0_\mu^Q | 0_\mu^g \rangle}$$

$$C_{BB}^{\tilde{s}} = \frac{\langle 0_\mu^g | 1_\mu^B \rangle \langle 1_\mu^B | 0_\mu^g \rangle}{\langle 0_\mu^g | 0_\mu^B \rangle \langle 0_\mu^B | 0_\mu^g \rangle} \tag{7}$$

$$C_{QB}^{\tilde{s},\tilde{a}} = \frac{\langle 0_\mu^g | 1_\mu^Q \rangle \langle 1_\mu^Q | 1_\mu^B \rangle \langle 1_\mu^B | 0_\mu^g \rangle}{\langle 0_\mu^g | 0_\mu^Q \rangle \langle 0_\mu^Q | 0_\mu^B \rangle \langle 0_\mu^B | 0_\mu^g \rangle} + \tilde{C}_{QB}^{\tilde{s},\tilde{a}}$$

$\tilde{\nu}_\mu$ is the wave number of the representative phonon.

$\langle 0^g| = \langle 0\ 000|$ is the vibronic wave function of the electronic ground state with no vibration excited

$\langle 1_\mu^e| = \langle 0\ 01_\mu^e 0|$ is the vibronic wave function of the electronic state $|e\rangle$ (Q, B) with one representative vibration excited.

$\tilde{C}_{QB}^{\tilde{s},\tilde{a}}$ is a term resulting from the fact that the Q_{01}-band, which becomes allowed optically by vibronic coupling of the Q- and B-state with B_{1g}, A_{2g}, B_{2g}-modes in the cyclic polyene model, contributes to Raman scattering. The sum over Γ runs over the modes A_{1g}, B_{1g}, B_{2g}. $\hat{\beta}_{\text{dist}}$ is normalized on the 0-0 overlap product. Thus, we have introduced four new parameters $C_{QQ}^{\tilde{s}}$, $C_{QB}^{\tilde{s},\tilde{a}}$, and $C_{BB}^{\tilde{s}}$ into our fit. These have shown to be sufficient to obtain good fits also for the data observed in *oxy*Hb and will also be reported in the future.

From Eq. (6) the DPR has been calculated accordingly to the classical theory of Placzek (1934):

$$\varrho = \frac{I_\parallel}{I_\perp} = \frac{3\,\gamma^2 + 5\,\beta^a}{10\,\beta^s + 4\,\gamma^2}. \tag{8}$$

β^s, γ^2 and β^a are related to the isotropic, anisotropic and antisymmetric parts S^0, S^s and A of the polarizibility tensor by

$$\begin{aligned} \beta^s &= Tr(S^0 S^0) \\ \gamma^2 &= Tr(S^s S^s) \\ \beta^a &= -Tr(AA^+) \\ S_{ij}^0 &= \frac{1}{3}(\beta_{xx} + \beta_{yy} + \beta_{zz})\,\delta_{ij} \\ S_{ij}^s &= \frac{1}{2}(\beta_{ij} + \beta_{ij}) - S_{ij} \\ S_{ij}^a &= \frac{1}{2}(\beta_{ij} - \beta_{ji})\,. \end{aligned} \tag{9}$$

Table 2 lists the meaning of the complete set of our fitting parameters. We try to reproduce our experimental DPR and EPS dispersion curves with a minimal number of these constants.

Table 2. Physical meaning of the various constants in Eq. (6)

Fitting constant	Function
$\alpha_{e,s}$	Complex constants for each tensor T of the representation related to:
α_{BB}^{Γ}	Soret transition
α_{QB}^{Γ}	Herzberg Teller coupling
α_{QQ}^{Γ}	α-transition
$C_{e,s}$	Ratios of FC overlap integrals related to:
C_{BB}	Soret transition
C_{QB}	Herzberg Teller coupling
C_{QQ}	α-transition
$\tilde{\nu}_{\mu_{1g}}$	Wave number of the representative vibrational phonon
γ^{es}	Electronic half-width of the
γ^{Q}	α-band
γ^{B}	Soret band

The expression in Eq. (6) is derived with the assumption that all the molecules contributing to the Raman scattering are identical also with respect to their distortions δQ_j. In haemoglobin, however, this is not the case, since the tetramer consists of α- and β-chains and the environment of the haem is different in the crevices of the α and β helices, respectively (Ten Eyck 1979). Therefore, the question arises whether calculations of ϱ and $I_{\parallel}$, $I_{\perp}$ are still meaningful if one uses Eq. (6).

Since the DPR and the excitation profiles are only dependent on the squares of the tensor components, and different molecules contribute incoherently, one gets an apparent tensor $\hat{\beta}^{(*)}$ given by

$$|\hat{\beta}_{\varrho\sigma}^{*}|^2 = \frac{1}{2}|\hat{\beta}_{\varrho\sigma}^{(\alpha)}|^2 + \frac{1}{2}|\beta_{\varrho\sigma}^{(\beta)}|^2 . \tag{10}$$

$\beta^{(\alpha)}$, $\beta^{(\beta)}$ are the tensor components of the two different molecules. Simple arithmetic shows that $|\hat{\beta}_{\varrho\sigma}^{*}|$ has the same functional structures as $\hat{\beta}_{\text{dist}}$ from Eq. (6). The fitting constants corresponding to α_{es}^{Γ} in Eq. (6), which are proportional to δQ_j are now related to an effective distortion $\delta Q_{es}^{(e)}$ due to both different molecules given by

$$|\delta Q_{es}^{(e)\Gamma}| = \sqrt{\frac{1}{2}|\delta Q_{es}^{(\alpha)\Gamma}|^2 + \frac{1}{2}|\delta Q_{es}^{(\beta)\Gamma}|^2} . \tag{11}$$

With these considerations the fitting procedure of Eq. (6) is still meaningful if molecules of different distortions contribute to the Raman intensity.

This approach in a somewhat more complex form will be used in the interpretation of the pH-dependence of the fitting parameters α_{es}^{Γ}, which give information on the variation of solvent induced distortions of the haeme group.

The Fitting Program

For the computer fit we use a program of the CERN library called MINUITL, described by F. James and M. Roos (James 1972). This fitting program works as subroutine of a program, calculating with the expressions of Eq. (6) for the tensor components and using Placzek's (1934) theory for the DPR and $I_\perp$ and $I_\parallel$.

MINUITL is able to work with a maximum of 55 variable parameters to fit a given function of the variable $\varkappa_{es}$, containing those parameters as constant to a given set of experimental data. It uses three different minimizing subroutines SEEK, SIMPLX, and MIGRAD for the search of a local minimum of the corresponding $\varkappa^2$-function. SEEK is a Monte Carlo searching subroutine. SIMPLX a minimizing subroutine using a simplex method described by Nelder and Mead (James 1972). The most important subroutine is MIGRAD, which is based on a variable metric method by Fletcher and Powell (James 1972). The program is able to draw a two-dimensional projection of the computed minimum. This gives good information about the quality of the fit.

Experimental

Human adult haemoglobin was prepared from freshly drawn blood standard procedures described by Brunner et al. (1972). Deoxyhaemoglobin was prepared by addition of a sufficient amount of $Na_2S_2O_4$, triggering simultaneously the pH-value of the solution in the acid range. The pH-value of 7.6 was adjusted by dializing the deoxyhaemoglobin solution against a 0.4 M *tris* buffer. The concentration of the haemoglobin solution was determined by measuring the optical absorbance. The haemoglobin concentration is expressed in mol/l in monomer.

The exciting radiation was obtained from an argon-ion laser. The laser beam polarized perpendicularly to the scattering plane, was focused by a cylindrical lens onto a rectangular sample, which was situated in copper block for cooling (temperature $\sim$ 6° C). A polarizer between sample and entrance slit of the Czerny-Turner double monochromator enables one to measure the intensity of the two components perpendicular ($I_\perp$) and parallel ($I_\parallel$) to the scattering plane. To eliminate the different transmission of the spectrometer for the two components, a polarization scrambler is placed between polarizer and entrance slit. To obtain the excitation profiles of the Raman lines, we have taken into account the transmission dispersion of the polarizer and the spectrometer. The transmission of the polarizer has been measured with a Cary absorption spectrometer. The transmission of the Raman spectrometer was determined by measuring the Raman intensity of several lines of calcite and quartz, which have frequency independent Raman tensors and by correcting for the $\tilde{\nu}_R^{-4}$-frequency dependence.

The excitation profiles were obtained from the thus corrected Raman intensities by dividing by $\tilde{\nu}_R^4$.

A correction for absorption of the samples is not necessary since the extinction coefficient of the solution for the concentration of maximal 10^{-3} mol/monomer is in the order of 8 cm^{-1}. The length of the scattering volume imaged

to the entrance slit is about 100 μ, which is by a factor of 10 smaller than the half width penetration depth of the exciting radiation.

Results

Figures 1 and 2 show the DPR dispersion curves and the corresponding excitation profiles of the 1,355 cm^{-1} oxidation marker-line of the deoxyhaemoglobin spectrum for different pH-values in the physiological and acid region. The full lines give the results of the fitting procedure. For all pH-values, we obtain good agreement with the experimental data.

In the physiological region the DPR dispersion curve has a significant minimum-maximum structure in the pre-resonant region between Soret- and α-band. In this particular region, however, there is no detectable influence of the pH-value within the experimental error. In contrast to this in the acid region between pH = 4.5 and pH = 6.0 a strong variation of DPR and EPS results. In the acid region below pH = 4.0 the dispersion of the DPR is considerably reduced.

The Raman spectra in the acid region are still of high quality with a large signal to noise ratio. From this we conclude that no denaturation effects have occurred.

Table 3 presents the values of the fitting parameters α_{es}^{Γ}. For all pH values A_{1g} and B_{2g} constants are present. At pH 5.6 and 4.9, additional B_{1g}-terms arise from the fitting procedure. This set of constants is unambigous, because the quality of the fit deteriorates dramatically, if one choses one of the constants to be equal to zero.

Although we did not need the constants C_{es} for the fits, $|(0)\rangle \rightarrow |(1\,\mu)\rangle$ transitions of the Q-band may contribute to the scattering tensor. Eaton and Hochstrasser (1968) conclude from optical measurements at myoglobin crystals

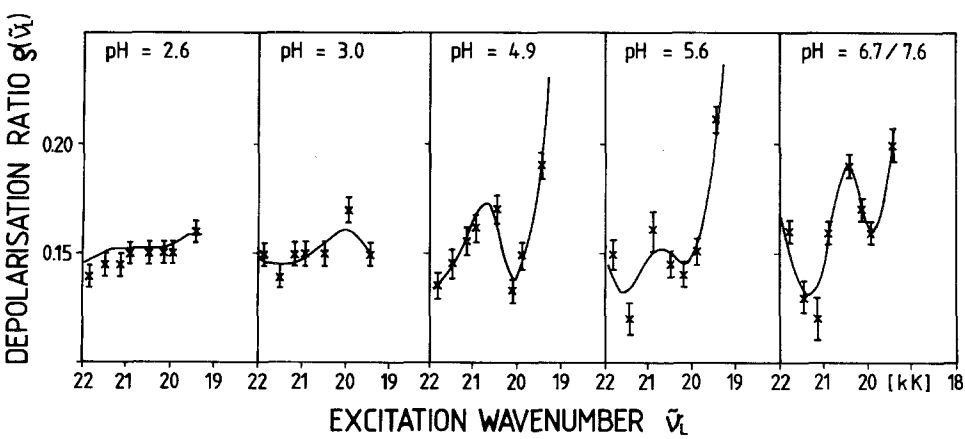

Fig. 1. DPR dispersion curves of the 1,355 cm^{-1} Raman line of the deoxyhaemoglobin spectrum for different pH-values of the solution

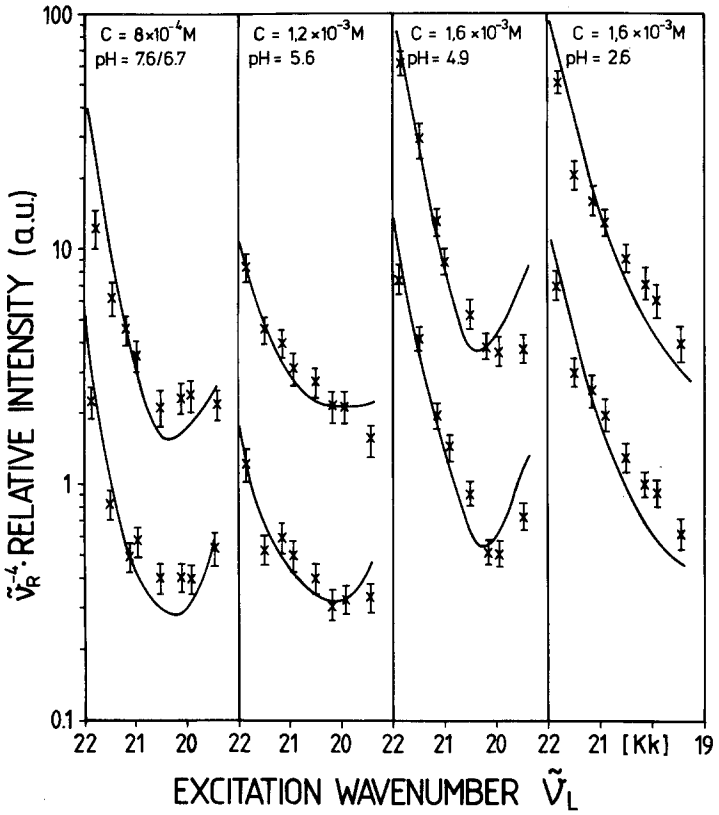

Fig. 2. EPS curves of the 1,355 cm^{-1} Raman line of the deoxyhaemoglobin spectrum for different pH-values of the solution

that the broad α-band in the spectra of haem proteins (*deoxy*Hb, *deoxy*Mb, MbCN) is dominated by the vibronic side band of the Q-transition.

One result is remarkable and requires further comment. All fitting constants α_{es}^{Γ} have to be taken as complex parameters. By using only real parameters in no case did we succeed to fit the experimental data, i.e., the DPR and EPS simultaneously. This is also true for DPR and EPS in *oxy*Hb, which are out of the scope of this report and will be published in a future paper. This is a rather surprising result, since all the electronic wave functions representing the basis for the calculation of the matrix elements in Eq. (5) may be chosen as real. This seems contradictory but a plausible explanation can be given.

The PNSF theory based on Loudon's approach is a strictly time-dependent perturbation theory, including the time dependence of the photon and the phonon field. In our introduction of the extra electronic levels associated with the creation of one phonon, we have used a time independent approach for simplicity. In the formulation of Loudon a fifth-order time-dependent contribution would have been necessary. This would have introduced new complex frequency denominators with resonance positions at the energies of the $|0_R, 0_\mu\rangle \rightarrow |0_R, 0_\mu\rangle$, $|0_R, 0_\mu\rangle \rightarrow |0_R, 1_\mu\rangle$ and the $|0_R, 0_\mu\rangle \rightarrow |1_R, 1_\mu\rangle$ transitions

Table 3. α_{es}^{Γ}-values of the 1,355 cm^{-1} Raman line of the deoxyhaemoglobin spectrum calculated by the fitting procedure

Tensor-comp.		pH				
		7.6/7.7	5.6	4.9	3.0	2.6
$Re\alpha^{A_{1g}}$	QQ	−1.4	1.22	2.46	2.04	0.79
	QB	–	–	–	–	–
	BB	3.8	1.50	1.01	4.08	2.98
$Re\alpha^{B_{1g}}$	QQ		−2.12	−0.24		
	QB		4.04	0.19		
	BB		1.75	2.72		
$Re\alpha^{B_{2g}}$	QQ	−2.0	1.05	3.16	0.32	–
	QB	6.4	0.25	−5.60	−0.87	−0.28
	BB	4.6	1.66	0.17	2.68	2.19
$Im\alpha^{A_{1g}}$	QQ	−0.5	0.38	1.12		
	QB	–	–	–	–	
	BB	–	−1.22	3.94		
$Im\alpha^{B_{1g}}$	QQ	–	–	−1.72		
	QB		5.16	−0.12		
	BB		–	–		
$Im\alpha^{B_{2g}}$	QQ		–	−1.49	−0.63	
	QB	6.40	0.68	−3.11	−1.41	
	BB		–	–	–	

of the Q- and B-bands respectively. μ refers to the occupations number of the phonon created in the optical transition; R refers to the Raman phonon. Schweitzer (1983) has shown numerically that Eq. (12) is in the wavelength region of our interest a good approach to the more complicated fifth-order formulation and the complex constants thus simulate higher-order time-dependent contributions.

Thus, our theoretical approach from the intellectual point of view may not seem convincing. It is, however, suitable to parametrize the extremely complex experimental data into numbers with a clear physical meaning, i.e., a scale of distortions from the ideal D_{4h}-symmetry of the molecule.

The applicability of our approach is supported by the work of S. el Naggar et al. (1983) who have measured DPR and EPS in solution and single crystals of *deoxy*Mb and ferric MbCN for both the lines at 1,355 and 1,584 cm. They thus obtain a set of seven independent DPR and EPS, which could be fitted simultaneously by using our approach.

Discussion

It is well known that the pH-value of the solution influences the oxygen binding of human haemoglobin. Perutz (1970) has shown that the binding of oxygen induces disruption of salt bridges between the subunits of the haemoglobin

tetramer. This leads to a discharge of protons. Otherwise a protonation of the titrable groups of His (H3), Val (NA2), His (G19) stabilizes these salt bridges, including a discharge of oxygen (alkaline Bohr effect). Thus, the titration of such Bohr groups is able to change the tertiary structure of the molecule and the properties of the haem groups. The kind of this pH-induced haem-apoprotein interaction, however, is unknown. In the acid region below pH = 6.0 the oxygen affinity increases with decreasing pH-value (acid Bohr effect). No satisfactory explanation for this phenomenon has yet been given. One would except, however, that protonation of titrable groups destabilizes the tetrameric *T*-structure of the haemoglobin molecule.

With this assumption we construct a simple model for calculating the pH-dependence of the tensor parameters α_{es}^{Γ} which are linearly dependent on the static distortions δQ_j of the haem group. The changes of oxygen affinity should be due to changes of the Fe^{++}-MO energies resulting from changes of the tertiary structure. These changes of Fe^{++} orbital energies arise if the porphyrin molecule is distorted by haem-apoprotein contacts which change upon changes of the titration of Bohr groups.

We assume that two different Bohr groups with mass action constants K_1 and K_2 are present. At a given pH-value molecules of different titration states are present. We classify these states $S_1 = (++)$, $S_2 = (+-)$, S_3 $(-+)$, and $S_4 = (-,-)$. + means that a proton is attached to Bohr group, − that a proton has been released. The number n_1 of each kind of molecules can be calculated by mass action law as a function n_1 (K_1, K_2, pH). The titration of each Bohr groups produces a specific distortion at the haem group which are superposed.

Analogous to the derivation of Eq. (11), this leads to the following expression for the effective constant $\alpha_{es}^{\Gamma_{\text{eff}}}$:

$$\begin{matrix}\text{Re}\\ \text{Im}\end{matrix}(\alpha_{es}^{\Gamma_{\text{eff}}}) = \begin{cases} \left\{\sum_{l=1}^{4} \frac{\eta_l}{N}\left[\left(\begin{matrix}\text{Re}\\ \text{Im}\end{matrix}(\eta_{es}^{\Gamma}\,\delta Q^{\Gamma_j})\right)^2 + \left(\begin{matrix}\text{Re}\\ \text{Im}\end{matrix}(\varepsilon_{es}^{\Gamma_R})\right)^2 \right.\right. \\ \qquad \left.\left. + \left(\begin{matrix}\text{Re}\\ \text{Im}\end{matrix}(\eta_{es}^{\Gamma})\begin{matrix}\text{Re}\\ \text{Im}\end{matrix}(\varepsilon_{es}^{\Gamma_R})\,\delta Q^{\Gamma_j}\right)\right]\right\}^{1/2} (\Gamma = \Gamma^R) \\ \left[\sum_{l=1}^{4} \frac{\eta_l}{N}\left(\begin{matrix}\text{Re}\\ \text{Im}\end{matrix}(\eta_{es}^{\Gamma})\,\delta Q^{\Gamma_j}\right)^2\right]^{1/2} (\Gamma \neq \Gamma^R) \end{cases} \tag{12}$$

where

$$\eta_{es}^{\Gamma} = \sum_j \langle g|R_Q|s\rangle \left\langle s\left|\frac{\partial^2 H}{\partial Q_R\,\partial Q_j}\Gamma_j\right|e\right\rangle\langle e|R_\sigma|g\rangle$$

$$\varepsilon_{es}^{\Gamma_R} = \langle g|R_Q|s\rangle\left\langle s\left|\frac{\partial H}{\partial Q_R}\right|e\right\rangle\langle e|R_\sigma|g\rangle$$

contain the matrix elements for electric dipol transitions from the ground state into the excited electronic states *e, s* and the vibronic-coupling element. Details of the simple but lengthy calculations are published by Schweitzer (1983).

Using pK_1, pK_2 and the terms in brackets as fitting parameters we are able to fit the α_{es}^{Γ} (pH)-diagrams of the 1,355 cm^{-1}-line of deoxyhaemoglobin. Figure 3 shows a good agreement of the fitting curves with the data points. The pK-values calculated from this procedure lie between 4.0 and 4.6 (pK_1) and between 5.3 and 5.8 (pK_2). From this we conclude that two titrable amino acid residues with $pK_1 = 4.3 \pm 0.3$ and $pK_2 = 5.4 \pm 0.3$ give rise to distortions of the haem group.

A possible interpretation of the pK_1 value can be given by referring to an earlier work of Lewis (1954). He has shown that the globin-haem complex of the deoxystate dissociates in the acid region between pH = 2.5 and pH = 4.5 with pK-value of 4.3. Thus, our pK_1-value may be identified with this process. In this case the small DPR dispersion at pH = 3.0 and 2.6 reflects the lack of distortions by haem-apoprotein contacts.

For the pK_2-value two possibilities are most likely. Resonant Raman measurements at $Hb^{III}F$ and $Mb^{III}F$ reported by Asher et al. (1981) as well as flash photolyse experiments by Doster et al. (1982) show that the distal histidine E7 titrates in the region between pH = 5.1 and pH = 5.7. A protonation of the imidazole group of this amino acid may influence the amino acid Val E11 via a H^+-bond. Val E11 is in van der Waals contact with the haem group (Ten Eyck 1979) and thus by this interaction the observed distortions may be induced. On the other hand myoglobin does not show any significant Bohr effect in the acid region at temperatures below 10° C (Antonini and Brunori 1971; La Mar et al. 1978), which is an argument against a dominant role of His E7 for the acid Bohr effect.

Perutz et al. (1980) have identified His (H21)β as the residue responsible for about half acid Bohr effect. The authors calculate a pK-value of 4.9 for

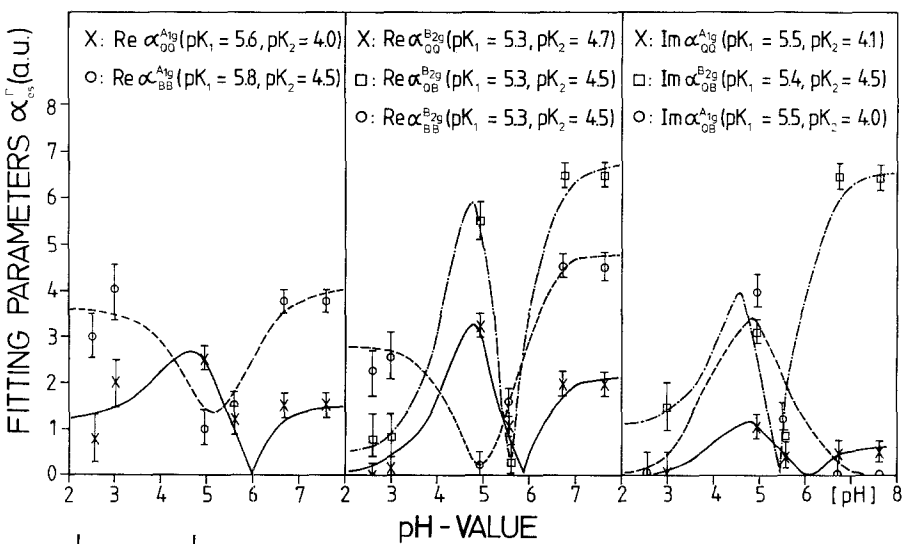

Fig. 3. $\left|\begin{matrix}\mathrm{Re}\\ \mathrm{Im}\end{matrix}\ \alpha_{es}(\mathrm{pH})\right|$-curves of the 1,355 cm^{-1} Raman line of the deoxyhaemoglobin spectrum for different pH-values of the solution

the deoxy state, which is close to the value we have observed. At present we cannot decide which of the two possibilities is realized.

The pK-values at the alkaline Bohr groups lie above 8.0 in the deoxy state (Matthew et al. 1979a and b; Soni and Kiesow 1977). Thus, most of these groups are protonated below pH = 7.6, and therefore one does not expect a significant pH-influence on the haem symmetry in the physiological region. This is reflected by the pH-dependence of the α_{es}^{Γ} (Fig. 1) in the region above pH = 6.0.

We summarize our results as follows:

1. Measurements and analysed DPR dispersion curves and excitation profiles of Raman lines are valuable tools for detecting symmetry-lowering distortions of the haem group.
2. Protonation of amino acid groups with pK-values of 4.3 and 5.4 induce distortions of the haem symmetry via haem-apoprotein contacts.
3. The dissociation of the haemoglobin complex between pH = 2.6 and 4.5 reduces the minimum-maximum structure of the 1,355 cm^{-1}-DPR curves in the pre-resonant region between α- and Soret band.

Acknowledgements. We would like to thank Professor Dr. A. Mayer for many discussions, Mr. G. Ankele for technical assistance and Mr. W. Spickermann from the Computer Center of the University of Wuppertal for good advice in relation to the fitting program of the CERN library.

References

Antonini E, Brunori M (1971) Hemoglobin and myoglobin in their reactions with ligands. North-Holland, Amsterdam, London

Asher SA, Adams ML, Schuster TM (1981) Resonance Raman and absorption spectroscopic detection of distal histidine-fluoride interactions in human methemoglobin fluoride and sperm Whale metmyoglobin fluoride: Measurements of distal histidine ionization constants. Biochemistry 20 : 3339–3346

Brunner H, Mayer A, Sussner H (1972) Resonance Raman scattering on the haem group of oxy- and deoxyhaemoglobin. J Mol Biol 70 : 153–156

Burke JM, Kincaid JR, Peters S, Gagne RR, Collman JP, Spiro TG (1978) Structure-sensitive resonance Raman bands of tetraphenyl and "Picket Fence" porphyrin-iron complexes, including an oxy hemoglobin analogue. J Am Chem Soc 100 : 6083–6088

Collins DW, Fitchen DB, Lewis A (1973) Resonant Raman scattering from cytochrome c: Frequency dependence of the depolarization ratio. J Chem Phys 59 : 5714–5718

Debois A, Lutz M, Banerjee R (1981a) Resonance Raman spectra of deoxyhemeproteins heme structure in relation to dioxygen binding. Biochim Biophys Acta 671 : 177–183

Debois A, Lutz M, Banerjee R (1981b) Protoheme conformations in low-spin ferrohemeproteins resonance Raman spectroscopy. Biochim Biophys Acta 671 : 184–192

Debois A, Lutz M, Banerjee R (1979) Low frequency vibrations in resonance Raman spectra of horse heart myoglobin. Iron-ligand and Iron-nitrogen vibrational modes. Biochemistry 18,8 : 1510–1518

Doster W, Been D, Bowne SF, Di Iorio EE, Eisenstein L, Frauenfelder H, Remisch L, Shyansunder E, Wintherhalter KH, Yu KT (1982) Control and pH dependence to heme proteins. Biochemistry 21 : 4831–4839

Eaton WA, Hochstrasser RM (1968) Single-crystal spectra of ferrimyoglobin complexes in polarized light. J Chem Phys 49 : 985–995

Henneker WH, Penner AP, Siebrand W, Zgierski MZ (1978a) Resonance Raman excitation profiles and depolarization dispersion curves, and their use in the analysis of vibronically coupled excited states. J Chem Phys 69 : 1704–1721

Henneker WH, Penner AP, Siebrand W, Zgierski MZ (1978b) Exactly solvable models for vibronic coupling in molecular spectroscopy. III. The pseudo Jahn-Teller effect. J Chem Phys 69 : 1884–1896

James F (1972) Function minimization. Proceedings of the 1972 CERN Computing and Data Processing School, Pertisau, Austria, 10–24 September 1972 (CERN 72–21)

Kincaid J, Stein P, Spiro TG (1979) Absence of heme-localized strain in T state hemoglobin: Insensitive of heme-imidazole resonance Raman frequencies to quaternary structure. Proc Natl Acad Sci 76 : 549–552

LaMar GN, Budd DL, Sick H, Gersonde K (1978) Acid Bohr effects in myoglobin characterized by proton NMR hyperfine shifts and oxygen binding studies. Biochim Biophys Acta 537 : 270–283

Lewis UJ (1954) Acid cleavage of heme proteins. J Biol Chem 205 : 109–117

Loudon R (1973) The quantum theory of light. Clarendon Press, Oxford

Matthew JB, Hanania GIH, Gurd FRN (1979a) Electrostatic effects in hemoglobin: Hydrogen ion equilibria in human deoxy- and oxyhemoglobin A. Biochemistry 18 : 1919–1927

Matthew JB, Hanania GIH, Gurd FRN (1979b) Electrostatic effects in hemoglobin: Bohr effect and ionic strength dependence of individual groups. Biochemistry 18 : 1928–1936

McClain WM (1971) Excited state symmetry assignment through polarized two-photon absorption studies of fluid. J Chem Phys 55 : 2789–2796

Mendelsohn R, Sunder S, Verma AL, Bernstein HJ (1975) Resonance Raman spectra of Cu-etioporphyrins I, I-meso-d_4, and IV. J Chem Phys 62 : 37–44

Nagai K, Kitagawa T, Morimoto H (1980) Quaternary structures and low frequency molecular vibrations of haems of deoxy and oxyhaemoglobin studied by resonance Raman scattering. J Mol Biol 136 : 271–289

Ondrias MR, Rousseau DL, Shelnutt JA, Simon SR (1982) Quaternary-transformation-induced changes at the heme in deoxyhemoglobins. Biochemistry 21 : 3428–3437

Perutz MF (1970) The Bohr effect and combination with organic phosphates. Nature 228 : 734–739

Perutz MF, Kilmartin JV, Nishikura K, Fogg JH, Butler PJG (1980) Identification of residues contributing to the Bohr effect of human haemoglobin. J Mol Biol 138 : 649–670

Peticolas WL, Nafie L, Stein P, Fanconi B (1970) Quantum theory of the intensities of molecular vibrational spectra. J Chem Phys 52 : 1576–1588

Placzek G (1934) Rayleigh-Streuung und Raman-Effekt. In: Marx E (ed) Handbuch der Radiologie, Bd 6. Akademische Verlagsgesellschaft, Leipzig

Plus R, Lutz M (1974) Study of band IV of porphyrin by resonance Raman spectroscopy. Spectrosc Lett 7 : 73–84

Scholler DM, Hoffmann BM (1979) Resonance Raman and electron paramagnetic resonance studies of the quaternary structure change in Carp hemoglobin. Sensitivity of These Spectroscopic Probes to Heme Strain. J Am Chem Soc 107 : 1655–1662

Schweitzer R (1983) Untersuchung von pH-induzierten Symmetrieverzerrungen der prosthetischen Gruppe in Hämoglobin durch resonante Ramanstreuung. Doctor Thesis, Bremen

Schweitzer R, Dreybrodt W, Mayer A, el Naggar S (1982) Influence of the solvent environment on the polarization properties of resonance Raman scattering in haemoglobin. J Raman Spectrosc 13 : 139–148

Shelnutt JA (1979) The Raman excitation spectra and absorption spectrum of a metalloporphyrin in an environment of low symmetry. J Chem Phys 72 : 3948–3958

Shelnutt JA, Rousseau DL, Friedman JM, Simon SR (1979) Protein-heme interaction in hemoglobin: Evidence from Raman difference spectroscopy. Proc Natl Acad Sci USA 76 : 4409–4413

Soni SK, Kiesow LA (1977) pH-dependent Soret difference spectra of the deoxy and carbonmonoxy forms of human hemoglobin and its derivatives. Biochemistry 16 : 1165–1170

Sunder S, Mendelsohn R, Bernstein HJ (1975) Resonance Raman spectra of Cu-1:3:5:7-tetramethyl porphin and Cu-1:2:3:4:5:6:7:8-octamethyl porphin. J Chem Phys 63 : 573–580

Ten Eyck LF (1979) Hemoglobin and myoglobin. In: Dolphin D (ed) The porphyrins, vol VII. Academic Press, New York San Francisco London

Tsubaki M, Srivastava RB, Yu NT (1982) Resonance Raman investigation of carbon monoxide bonding in (carbon monoxy) hemoglobin and -myoglobin: Detection of Fe-CO Stretching and Fe-C-O bending vibrations and influence of the quaternary structure change. Biochemistry 21 : 1132–1140

Valance WG, Strekas TC (1982) Low frequency resonance Raman spectra of ferrocytochrome c and liganded derivatives. Evidence of symmetry lowering in native ferrocytochrome c. J Phys Chem 86 : 1804–1808

Verma AL, Bernstein HJ (1974) Resonance Raman spectra of copper-porphin. J Chem Phys 61 : 2560–2565

Verma AL, Mendelsohn R, Bernstein HJ (1974) Resonance Raman spectra of the nickel, cobalt, and copper chelates of mesoporphyrin IX dimethyl ester. J Chem Phys 61 : 383–390

Zgierski MZ, Pawlikowski M (1978) Theory of depolarization dispersion of inversely polarized modes in heme proteins. Chem Phys Lett 57 : 438–441

Zgierski MZ, Pawlikowski M (1981) Multimode effects in resonance Raman excitation profiles 392 cm^{-1} fundamental of copper tetraphenyloporphyrin. Chem Phys Lett 78 : 451–455

Zgierski MZ, Pawlikowski M (1982) Depolarization dispersion curves of resonance Raman fundamentals of metalloporphyrins and metallophthalocyanines subject to asymmetric perturbations. Chem Phys 65 : 335–367

Zgierski MZ, Shelnutt JA, Pawlikowski M (1979) Interference between intra- and inter-manifold couplings in resonance Raman spectra of metalloporphyrins. Chem Phys Lett 68 : 262–266

Received September 20, 1983/Accepted December 13, 1983